1678–1689 *Nucleic Acids Research, 2005, Vol. 33, No. 5*
doi:10.1093/nar/gki313

Both RNase E and RNase III control the stability of *sodB* mRNA upon translational inhibition by the small regulatory RNA RyhB

Taras Afonyushkin, Branislav Večerek, Isabella Moll, Udo Bläsi and Vladimir R. Kaberdin*

Max F. Perutz Laboratories, Department of Microbiology and Immunobiology, University Departments at the Vienna Biocenter, Dr. Bohrgasse 9/4, A-1030 Vienna, Austria

Received January 24, 2005; Revised and Accepted March 2, 2005

ABSTRACT

Previous work has demonstrated that iron-dependent variations in the steady-state concentration and translatability of *sodB* mRNA are modulated by the small regulatory RNA RyhB, the RNA chaperone Hfq and RNase E. In agreement with the proposed role of RNase E, we found that the decay of *sodB* mRNA is retarded upon inactivation of RNase E *in vivo*, and that the enzyme cleaves within the *sodB* 5′-untranslated region (5′-UTR) *in vitro*, thereby removing the 5′ stem–loop structure that facilitates Hfq and ribosome binding. Moreover, RNase E cleavage can also occur at a cryptic site that becomes available upon *sodB* 5′-UTR/RyhB base pairing. We show that while playing an important role in facilitating the interaction of RyhB with *sodB* mRNA, Hfq is not tightly retained by the RyhB–*sodB* mRNA complex and can be released from it through interaction with other RNAs added in *trans*. Unlike turnover of *sodB* mRNA, RyhB decay *in vivo* is mainly dependent on RNase III, and its cleavage by RNase III *in vitro* is facilitated upon base pairing with the *sodB* 5′-UTR. These data are discussed in terms of a model, which accounts for the observed roles of RNase E and RNase III in *sodB* mRNA turnover.

INTRODUCTION

RNA processing and decay play important roles in controlling the level of particular transcripts under various growth conditions (1–3). In *Escherichia coli*, the degradation of mRNA is generally triggered by endoribonucleolytic cleavage, and the resulting intermediate products are further degraded by endo- and exoribonucleases [reviewed in (4,5)]. *E.coli* RNase E seems to initiate the decay of many, if not most, mRNAs (6–10). In some cases, the initial cleavage of transcripts can also be performed by RNase III (11). Although the subsequent steps of mRNA decay may sometimes require endoribonuclease RNase P (12), further degradation is believed to be accomplished by two major exoribonucleases, PNPase and RNase II, and oligoribonuclease (13). It has also been shown that auxiliary factors, such as RNA helicases and Hfq (14–18), that modulate RNA structure, can significantly affect mRNA stability.

Recent studies of the mechanisms, which are involved in cellular responses to numerous stress conditions, revealed that mRNA stability can be modulated by the action of small regulatory RNAs (sRNAs) (19). By base pairing with target mRNAs, sRNAs affect their translation and/or stability (20). In contrast to the regulation by classical antisense RNAs (21), base pairing of sRNA with their targets does not require a high degree of complementarity and, therefore, provides a possibility for sRNAs to affect multiple transcripts.

One of the best-studied *E.coli* sRNAs, RyhB, has been recently shown (17,20) to regulate the level of the *sodB* mRNA (Figure 1) encoding the iron superoxide dismutase [FeSOD (22)]. The *in vivo* level of RyhB is in turn controlled (23) by the transcriptional repressor Fur [ferric uptake regulator (24)], whose ability to repress RyhB transcription is iron-dependent. Similar to the action of other sRNAs (25–27), the interaction of RyhB with *sodB* mRNA is mediated by the *E.coli* RNA chaperone Hfq, which has been shown to induce structural rearrangements within the *sodB* 5′-untranslated region (5′-UTR) (Figure 1B) (28).

Although the formation of inhibitory complexes with sRNAs is believed to functionally inactivate their target mRNAs, the steps leading to subsequent disassembly and recycling of these complexes are poorly understood (29). The aim of this study is to recapitulate the functional inactivation of the *E.coli sodB* mRNA by the regulatory RNA RyhB *in vitro*.

*To whom correspondence should be addressed. Tel: +43 1 4277 54606; Fax: +43 1 4277 9546; Email: vladimir.kaberdin@univie.ac.at

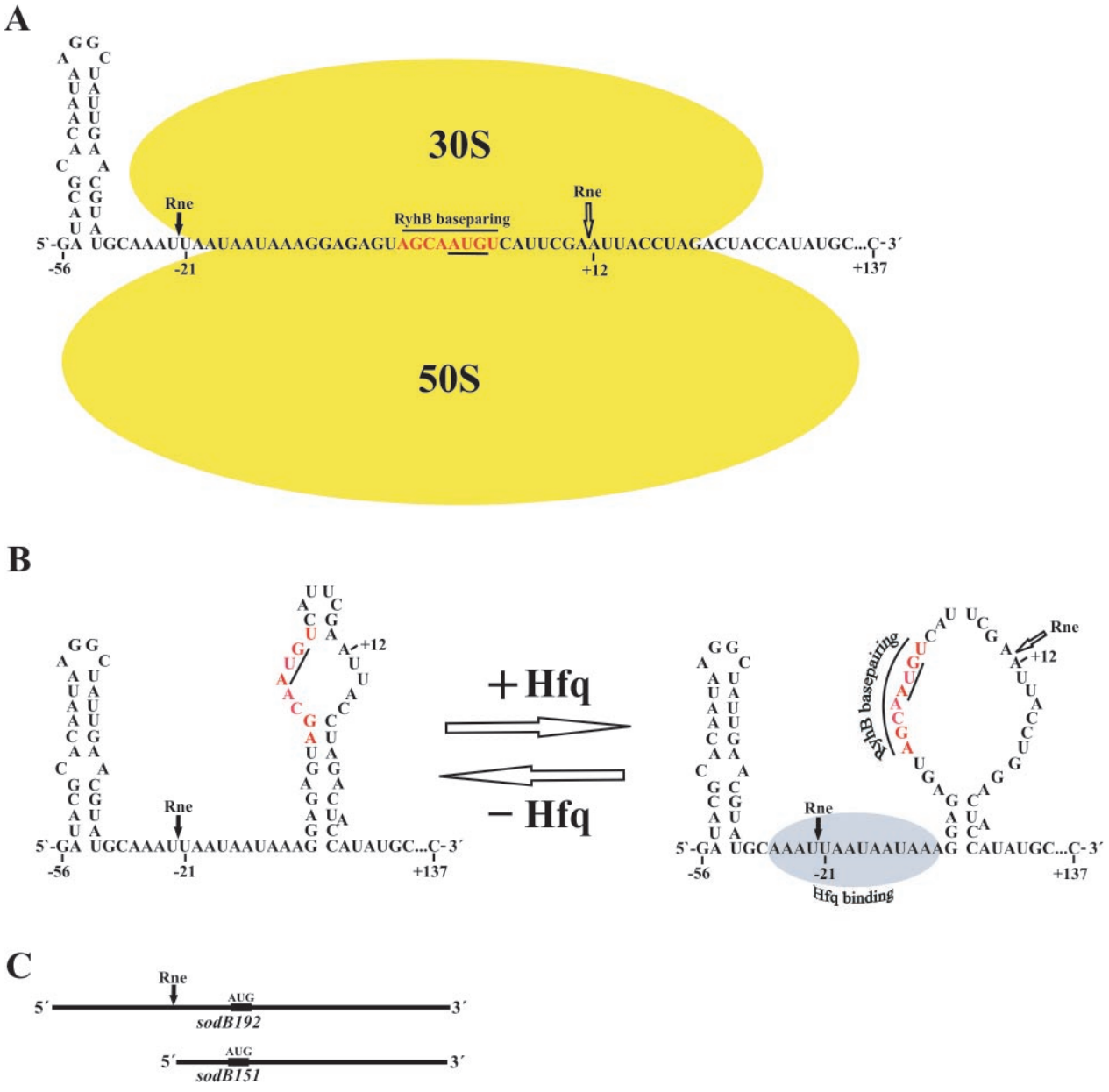

Figure 1. Alternative structures of the *sodB* 5′-UTR. (**A**) 30S ribosome subunit binding and subsequent formation of the translation initiation complex is believed to limit the access of Hfq, RyhB and/or RNase E (Rne) to the 5′ end of the *sodB* transcript. (**B**) In the absence of translation, the *sodB* 5′-leader apparently forms two alternative structures that were previously characterized by Geissman and Touati (28). The transition between these alternative structures is mediated by Hfq and determines the ability of the *sodB* mRNA to base pair with the small regulatory RNA RyhB (28). Indicated are two regions, which interact with Hfq and base pair with RyhB, respectively. The start codon of the *sodB* mRNA is underlined. The major RNase E cleavage site (black arrow) and an extra RNase E site (open arrow), which becomes available upon RyhB binding, were mapped during the course of this work (for details, see Figure 3). (**C**) The bars schematically depict *sodB192* and *sodB151* mRNAs. The positions of the initiation codon (AUG) and the position of the 5′ terminal RNase E cleavage site are indicated by black boxes and by an arrow, respectively.

MATERIALS AND METHODS

Bacterial strains, plasmids, media and growth conditions

The following *E.coli* strains were used in this study: N3433 [*rne*$^{+}$ (30)], N3438 [*rne*-3071, *recA* (31)], SDF204 [W3110 *rnc*$^{+}$ *TD1–17*::Tn*10* (32)] and SDF205 [*W3110 rnc105 TD1–17*::Tn*10* (32)]. The *E.coli* strains were grown in Luria–Bertani (LB) medium at 28°C.

To construct plasmid pUsod, the DNA fragment corresponding to the entire *sodB* gene was amplified from chromosomal DNA of *E.coli* strain MC4100 (33) by PCR using the primers SODBfw (5′-GCTCTAGA**TAATACGACTCACTATAG**ATACGCACAATAAGGCTATTGTACGTATG) containing extra nucleotides corresponding to the T7 promoter (in bold) (34) and an XbaI site (underlined) and SODBrev (5′-CGGGATCCGGATGCGGCGA-GTGCCTTATCC)

containing a BamHI site (underlined). The PCR product was cleaved with XbaI and BamHI and ligated into plasmid pUC18 (35) digested with the same endonucleases. The plasmid pURyhB (17) was used for RyhB RNA synthesis.

In vitro synthesis and labelling of RNA and single-stranded DNA

The 204 nt long single-stranded anti-*sod* DNA, containing the region complementary to the first 182 nt of *sodB* mRNA, was amplified using the XbaI-linearized plasmid pUsod and the 5′-[^{32}P]end-labelled primer Sod-rev (5′-CAGGTTGTTCAGGTTAGTGAC) by an asymmetric PCR, and then gel-purified. RyhB RNA was transcribed from HindIII-linearized plasmid pURyhB (17) using T7 RNA polymerase. The *sodB192* mRNA (Figure 1C), containing the *sodB* 5′ untranslated region and part of the coding region (nucleotides −55 to +137) and one G nucleotide at the 5′ end, was transcribed from *Asp*718I-linearized plasmid pUsod. The *sodB151* mRNA (Figure 1C), containing the truncated *sodB* 5′ untranslated region and part of the coding region (nucleotides −21 to +127) and three extra G nucleotides at the 5′ end, was transcribed using PCR-amplified SodB2 template. Plasmid pUsod was used for the amplification of SodB2 template with the following primers: 5′-AATTAATACGACTCACTATAGGGTAATAATAAAGGAGAGTAGCAA TG-TCATTCG (forward primer) and 5′-CAGGTTGTTCAGGTTAGTGAC (reverse primer). Underlined nucleotides correspond to the T7 RNA polymerase promoter (34). The RNAs were synthesized using the MEGAscript T7 kit (Ambion), gel-purified and 5′ end-labelled as described previously (36).

Northern blot analysis

Strains were grown at 30°C up to an OD_{600} of 0.4, and then the temperature was shifted to 44°C for 10 min before the addition of rifampicin (0.25 mg/ml). In some experiments (for details, see Figure legend 2), LB medium was also supplemented with 250 μM $FeSO_4$ that was added 16 min before rifampicin treatment. Total RNA was prepared from aliquots of the cultures withdrawn at various times using the hot phenol method (37). The RNA samples were fractionated on 4–8% polyacrylamide gels, transferred to Zeta-Probe membranes (Bio-Rad), using the Trans-Blot SD Semi-Dry Transfer Cell (Bio-Rad), and then separately hybridized with [^{32}P]labelled RNA probes specific for *sodB* mRNA, RyhB RNA or 5S rRNA as described previously (17). The signal intensities obtained with the radioactively labelled probes were quantitated on a PhosphorImager (Molecular Dynamics). The relative amount of *sodB* mRNA and RyhB at each time point was calculated by normalizing their signals to 5S rRNA signal.

Gel shift assays–western blot analysis

Aliquots containing 100 fmol of 5′-[^{32}P]labelled RNA were incubated for 10 min at 37°C with or without the addition of Hfq, which was purified as described by Vassilieva *et al*. (38), and unlabelled RNAs (as indicated in the Figure legends 4 and 5) in 10 μl binding buffer (10 mM Tris–HCl, pH 7.5, 5 mM magnesium acetate, 100 mM NH_4Cl and 0.5 mM DTT). After cooling on ice and addition of glycerol to a final concentration of 5%, the samples were loaded on a non-denaturing 4% polyacrylamide gel. Electrophoresis was performed in 0.5× TBE buffer at 40 V for 10–16 h, and the radioactive bands were visualized using a PhosphorImager (Molecular Dynamics). Thereafter, the gel was electroblotted onto Immobilon-P membrane (Millipore). The blotting was carried out in TBE buffer at 200 V for 30 min. After blotting, the membranes were blocked in 10% non-fat dry milk suspension and probed with anti-Hfq antibodies followed by development using the enhanced chemiluminescence detection kit (Amersham) as recently described (17).

RNase E cleavage of *sodB192* RNA

Aliquots containing 100 fmol of 5′-[^{32}P]labelled RNA were incubated for 10 min at 37°C in binding buffer (10 mM Tris–HCl, pH 7.5, 5 mM magnesium acetate, 100 mM NH_4Cl and 0.5 mM DTT) in the presence or absence of Hfq and unlabelled RNAs as indicated in Figure legend 3. Then, 20 ng of Rne498 (39) or 150 ng of degradosome (40) were added, and aliquots withdrawn at various time points were further extracted with phenol, mixed with an equal volume of loading dye solution (90% formamide, 0.5 mM EDTA, 0.025% xylene cyanol FF and 0.025% bromophenol blue), and then fractionated on 8% polyacryamide gels containing 8 M urea. The cleavage sites for RNase E and RNase III were mapped using endoribonuclease T1 and nuclease S1 digests of the corresponding RNAs. Briefly, 200 fmol of 5′-[^{32}P]labelled RNA were incubated with 4 U of ribonuclease S1 (MBI Fermentas) in 1× S1 buffer (MBI Fermentas) at 70°C for 1–8 min or with 0.1 U of ribonuclease T1 (MBI Fermentas) in 1× AT buffer (10 mM Tris–HCl, pH 7.5, 10 mM $MgCl_2$) at 37°C for 1–8 min.

RNase III cleavage of RyhB

Aliquots containing 40 fmol of 5′-[^{32}P]labelled RNA were pre-incubated with 6-fold molar excess of Hfq for 5 min at 37°C in 1× RNase III buffer (Ambion) in the absence or presence of increasing quantities of unlabelled *sodB192* RNA as indicated in Figure legend 7. Subsequently, 0.1 U of RNase III (Ambion) was added, and aliquots withdrawn at various time points were further extracted with phenol, mixed with an equal volume of loading dye solution (90% formamide, 0.5 mM EDTA, 0.025% xylene cyanol FF and 0.025% bromophenol blue), and then fractionated on a 6% polyacryamide gels containing 8 M urea.

Toeprinting assay

The toeprinting assays were carried out using 30S ribosomal subunits and $tRNA^{fMet}$ as described previously (41). The 5′-[^{32}P]labelled *sodB*-specific oligonucleotide Sod-rev (5′-CAGGTTGTTCAGGTTAGTGAC) complementary to nucleotides +137 to +117 of the *sodB* mRNA was used as a primer for cDNA synthesis in the toeprinting reactions. The *sodB192* RNA annealed to the primer was separated from free oligonucleotides on a MicroSpin G-50 column according to the manufacturer's instructions (Amersham Biosciences). An aliquot of 0.04 pmol of *sodB192* mRNA annealed to Sod-rev oligo was pre-incubated at 37°C for 5 min without or with 0.5 pmol of 30S subunits and 10 pmol of $tRNA^{fMet}$.

To compare the affinity of the 30S subunits for *sodB192* RNA and its truncated version *sodB151* RNA, increasing amounts of either *sodB192* or *sodB151* mRNA were added to the reaction mixtures after the annealing step before the

addition of 30S subunits, as indicated in the legend to Figure 3. The rationale was that the RNA with a higher affinity for 30S ribosomal subunit would compete with the *sodB192* RNA annealed to the 5′-[^{32}P]labelled oligonucleotide Sod-rev and, therefore, would reduce the toeprint signal more efficiently than the mRNA with a lower affinity.

RESULTS AND DISCUSSION

RNase E- and RNase III-dependence of *sodB* mRNA decay *in vivo*

Previous work has shown that the steady-state level of *sodB* mRNA is dependent on the *E.coli* chaperone Hfq, the small regulatory RNA RyhB, the transcriptional regulator Fur as well as on RNase E (17,42). To differentiate between direct and indirect roles of RNase E in determining the stability of the *sodB* transcript, northern blot hybridization to a [^{32}P]labelled riboprobe complementary to *sodB* mRNA was used to detect the full-length transcript in wild-type *E.coli* cells as well as in an *rne^{ts}* mutant strain at the non-permissive temperature after rifampicin treatment (Figure 2A). Both measurements were performed not only when *E.coli* cells were cultivated in medium with low or moderate iron content (LB) [i.e. under conditions leading to the coupled decay of the *sodB* and RyhB transcripts (42)] but also under conditions (LB + 250 μM $FeSO_4$) that should increase the concentration of activated Fur, the repressor of RyhB transcription (23). The latter was performed with the rationale to monitor the RyhB-independent decay of *sodB* mRNA. In both the cases (see Figure 2A and B), the decay of *sodB* mRNA was retarded upon inactivation of RNase E, thus suggesting that the RyhB-dependent (Figure 2A) as well as RyhB-independent (Figure 2B) decay of this transcript is mediated by RNase E. Nevertheless, none of the degradative intermediates could be detected in addition to the full-length species (data not shown), which may not be surprising because many *E.coli* mRNAs are known to decay without any detectable accumulation of intermediate products.

The same probe was also used to compare the rates of *sodB* mRNA decay in the wild-type and its isogenic *rnc* mutant lacking functional RNase III (Figure 2C and D). Interestingly, the RyhB-dependent decay of *sodB* mRNA was more efficient in the *rnc* mutant when compared with the wild-type strain (Figure 2C), suggesting that RNase III does not cleave this transcript *in vivo* but instead may affect the decay of this mRNA indirectly, e.g. by changing the steady-state level of RyhB. Consistently, the rate of *sodB* mRNA decay at reduced levels of RyhB was found to be the same in the wild-type and *rnc* mutant strains after 8 min of rifampicin treatment (Figure 2D). Given that the addition of $FeSO_4$ does not eliminate RyhB immediately (data not shown), RyhB apparently affects *sodB* mRNA decay during the initial period (from 0 to 8 min), thereby resulting in different decay rates observed in these strains at early time points (Figure 2D).

RNase E cleavage of *sodB* mRNA *in vitro*

The RNase E-mediated degradation of *E.coli* mRNAs is usually initiated within their 5′-UTRs, which are normally not protected by ribosomes and, therefore, serve as primary targets for RNA-binding proteins and endonucleases. To test whether RNase E also cleaves within the 5′-UTR of the *sodB* transcript, we separately incubated 5′ end-labelled *sodB192* RNA, which corresponds to nucleotide −56 to +136 of *E.coli sodB* mRNA (see Figure 1C), with affinity-purified RNase E (Rne498, residues 1–498) and *E.coli* degradosome (Figure 3A and B, respectively). As shown in Figure 3, RNase E cleavage of *sodB192* occurred at position U_{-21}, and the cleavage efficiency at this site was decreased in the presence of Hfq (Figure 3A, lanes 13–15). The latter is consistent with the previously documented ability of Hfq to bind in close vicinity of RNase E cleavage sites, thereby protecting RNase E substrates from the nuclease activity of this enzyme (15).

Moreover, we found that the structural changes, which are induced in the 5′-UTR of sodB mRNA upon binding to the regulatory RNA RyhB (28), affect the cleavage pattern. As shown in Figure 3A (compare lanes 18–20 with lanes 13–15) and Figure 3B (compare lanes 8–10 with lanes 3–5), an additional RNase E cleavage site was mapped downstream of the translational start, namely at position A_{+12} (Figure 3D). This observation suggests that base pairing with RyhB, which stimulates RNase E cleavage downstream of the start codon (see also Figure 1A), can trigger another pathway for sodB mRNA turnover *in vivo*.

RNase E cleavage within the 5′-UTR of *sodB* mRNA decreases its affinity for Hfq and ribosomes

Given that the *sodB* 5′-UTR is the location of the Hfq (28) and ribosome binding sites, we next investigated whether RNase E cleavage at the 5′ end of the *sodB* mRNA (see Figure 1B) leads to functional inactivation of the transcript, i.e. whether the truncated form of the *sodB* mRNA generated by cleavage at position U_{-21} (Figure 1C, *sodB152*) is still able to bind Hfq and to interact with 30S ribosomes. First, the affinity of *sodB192* and its truncated form *sodB151* to Hfq was compared by means of gel-shift assays. As shown in Figure 4A, although both [^{32}P]labelled transcripts (*sodB192* and *sodB151*) can bind Hfq, the truncated form (*sodB151*) has lower affinity. This suggested that the 5′ terminal hairpin structure facilitates Hfq binding. Likewise, the presence of this structure appears to confer higher affinity for ribosomes. This was revealed by comparing the ability of both transcripts (*sodB192* and *sodB151*) to interfere with translation inhibition on *sodB192* RNA (Figure 4B and C). As shown by toeprint analysis (Figure 4B), *sodB151* RNA was required in higher concentrations than *sodB192* RNA to achieve the same inhibitory effect on ribosome binding (Figure 4C).

Analysis of Hfq binding to and recycling from the RyhB–*sodB* 5′-UTR complex

Previous work has suggested that Hfq binding induces structural changes within the 5′-UTR of the *sodB* transcript, which facilitate base pairing with the small regulatory RNA RyhB (28). To study in more detail the composition of the inhibitory complex formed between RyhB and *sodB* mRNA, we employed gel-shift assays. Radioactively labelled *sodB192* RNA (Figure 1C) was incubated with increasing amounts of RyhB in the absence (Figure 5A, lanes 2–5) or presence (Figure 5A, lanes 7–10) of Hfq, and the resulting complexes were analysed on a native polyacrylamide gel. As anticipated,

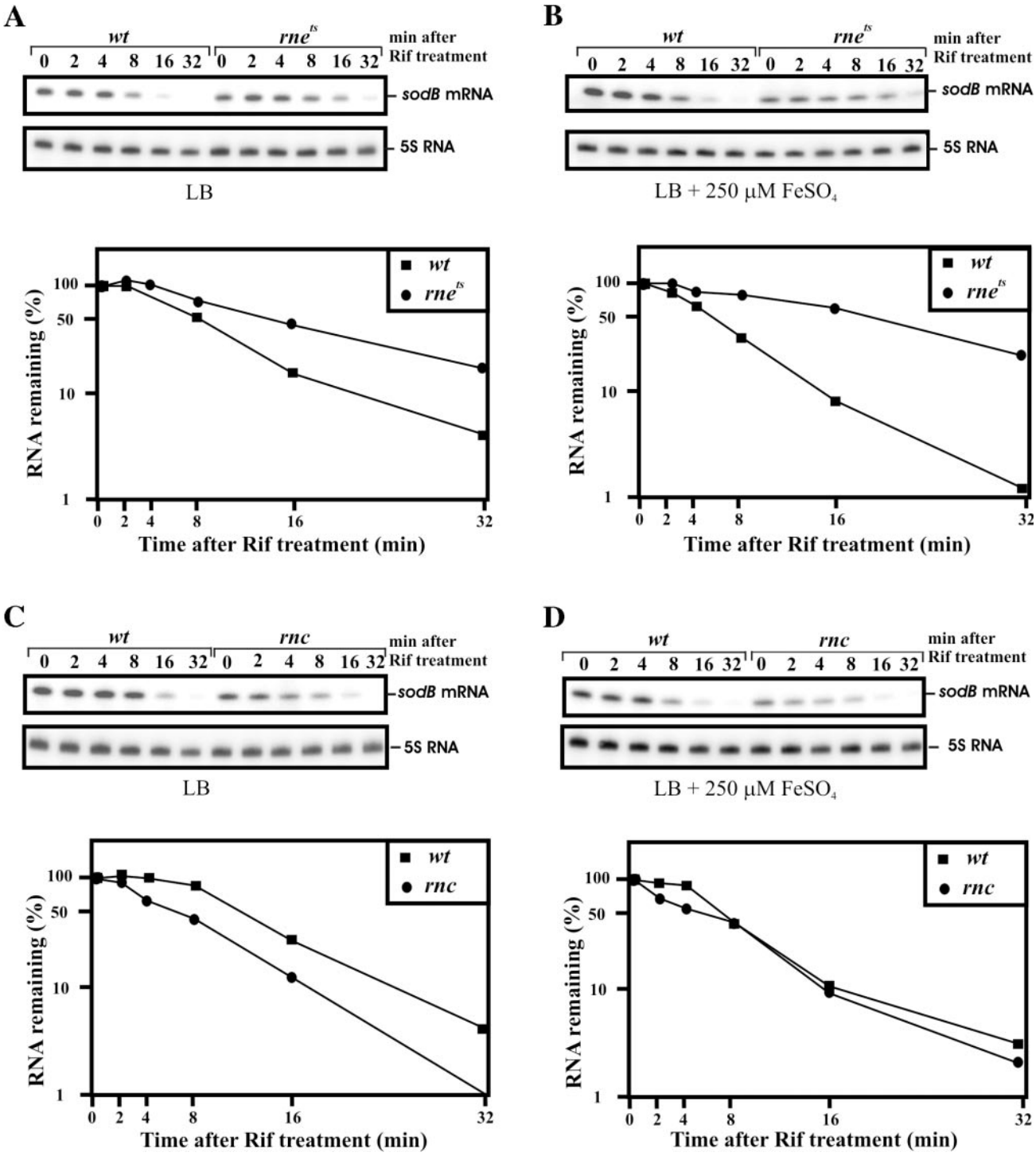

Figure 2. RNase E- and RNase III-dependence of *sodB* mRNA stability *in vivo*. *E.coli* strains and isogenic RNase E (*rne*^{ts}) and RNase III (*rnc*) mutants were grown either in LB medium (LB) or in LB medium supplemented with 250 μM $FeSO_4$ (LB + 250 μM $FeSO_4$) before rifampicin treatment, thereby favouring either RyhB-dependent (**A** and **C**) or RyhB-independent (**B** and **D**) *sodB* mRNA decay, respectively. RNA samples prepared from the above cultures before and after rifampicin treatment at the times indicated on top were analysed by northern blotting using probes specific for the *sodB* transcript and 5S rRNA. The latter was employed as an internal standard for normalization of *sodB*-specific signals. The graph at the bottom of each panel shows the relative amount of *sodB* mRNA remaining at each time point as determined by phosphorimaging, and plotted as a function of time.

base pairing of RyhB with *sodB192* RNA is strongly facilitated by Hfq. To test whether the resulting complex also contained Hfq, selected samples, which are shown in lanes 1, 6 and 10 of Figure 5A, were resolved on a separate gel, and the gel was blotted onto a PVDF membrane followed by probing with anti-Hfq antibodies (Figure 5B). As revealed by immunodetection, Hfq was part of the complex (marked by asterisks) formed by the base paired RNAs. *Vice versa*, labelling of

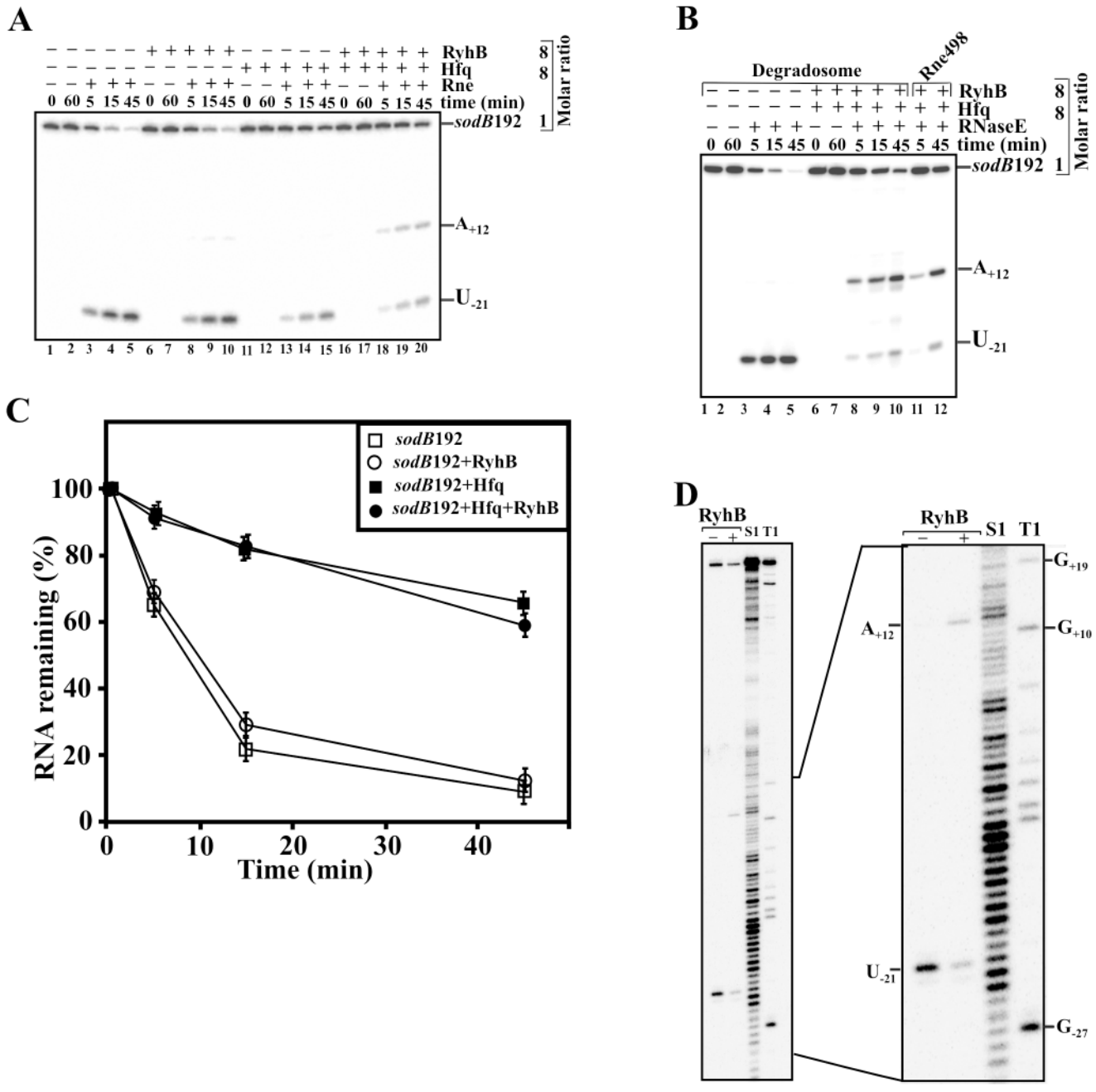

Figure 3. RNase E cleavage within the *sodB* 5′-UTR. 5′-[^{32}P]labelled *sodB192* was incubated either with RNase E polypeptide (Rne498, residues 1–498) or with RNA degradosome (40) in the presence or absence of Hfq and RyhB at 37°C (**A** and **B**, respectively). Aliquots were withdrawn at the times indicated above each lane, phenol extracted and analysed on an 8% sequencing gel. The graph on (**C**) shows the relative amount of s*odB192* mRNA remaining at each time point of (A) as determined by phosphorimaging and plotted as a function of time. (**D**) Mapping of the RNase E cleavage sites within the *sodB* 5′-UTR in the presence (+) or absence (−) of RyhB. The molar ratio of Hfq-hexamer:RyhB:*sodB192* was 8:8:1, respectively. The precise position of RNase E cleavage sites was determined from concomitantly run S1 and T1 digests of the same RNA.

RyhB confirmed that base pairing with *sodB192* is inefficient in the absence of Hfq (Figure 5C, compare lanes 2–5 with lane 7). Moreover, by the addition of increasing amounts of *sodB192* to the preformed ternary complex containing both RNAs and Hfq (lane 7), Hfq was apparently released from the ternary complex (lanes 8–10), resulting in a species (indicated by a single circle) that migrates at the position of the binary RyhB–*sodB192* complex. Therefore, although Hfq-mediated base pairing of sRNAs with their target does not simultaneously result in its release from the complex, these data might suggest that Hfq recycling occurs via interactions with other Hfq ligands.

RNase E-independent and RNase III-dependent decay of RyhB *in vivo*

Masse and Gottesman (20) have recently shown that inactivation of RNase E results in an increase in the steady-state level

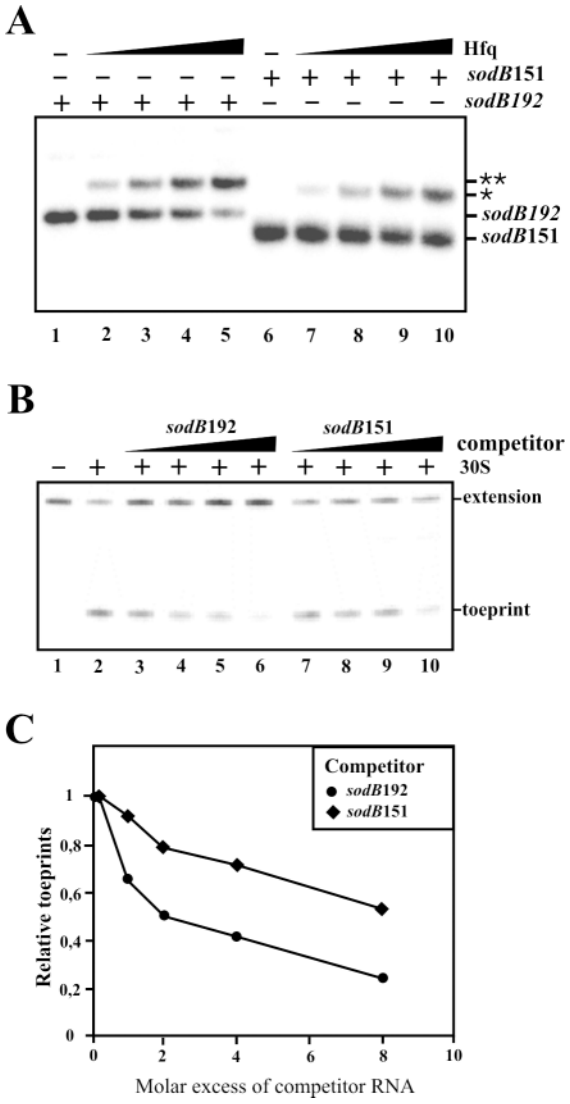

Figure 4. Effect of the 5′ terminal stem–loop structure on the affinity of the *sodB* 5′-UTR for Hfq and ribosomes. (**A**) 5′ end-labelled *sodB192* and *sodB151* RNAs were incubated alone (lanes 1 and 6) or with increasing amounts (2-, 4-, 6- and 8-fold molar excess) of Hfq-hexamer (lanes 2–5 and 7–10, respectively), and the resulting mixtures were then analysed on a 6% native gel. The positions of free *sodB151* and *sodB192* RNAs as well as their complexes with Hfq (single and double asterisks, respectively) are indicated. (**B**) Differential decrease of 30S ribosome binding to *sodB192* mRNA by *sodB192* and *sodB151* competitor RNA, respectively. The *sodB192* RNA pre-annealed to the 5′ end-labelled primer was incubated with 30S ribosomal subunits in the presence of increasing amounts (1-, 2-, 4- and 8-fold molar excess) of competitor RNAs (*sodB192* and *sodB151*, respectively). Translation inhibition complex formation was further analysed by primer extension as described in Materials and Methods. (**C**) Relative toeprints obtained on *sodB192* RNA [see (B)] using *sodB192* and *sodB151* RNA as competitors, respectively. The relative toeprints (%) were calculated as described by Hartz *et al*. (58) after quantitation of the toeprint and extension signals using the equation: [toeprint signal/(toeprint signal + extension signal)].

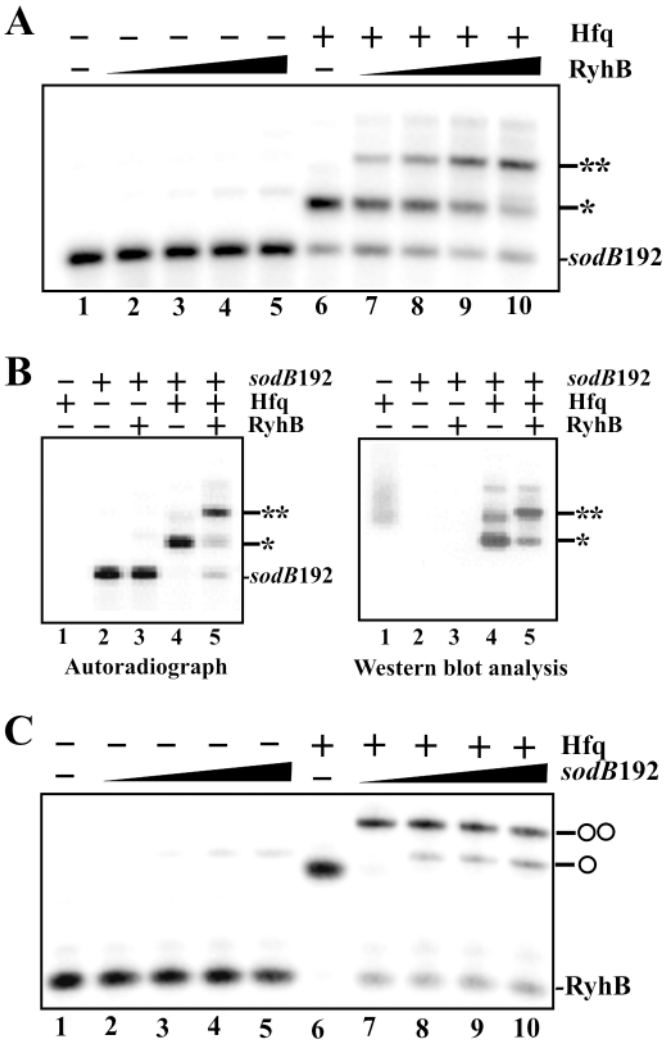

Figure 5. Hfq recycling from the RyhB–*sodB* 5′-UTR complex is facilitated by a molar excess of target RNA. (**A**) Radioactively labelled *sodB192* RNA (nucleotides −56 to 136) was incubated alone (lane 1) or with increasing quantities of RyhB (1-, 2-, 4- and 8-fold molar excess) in the absence (lanes 2–5) or presence (lanes 6–10) of Hfq (the ratio of *sodB192* RNA to Hfq-hexamer was 1:1), and the resulting complexes were analysed on a 6% native polyacrylamide gel as described in Materials and Methods. Single and double asterisks indicate the *sodB192*–Hfq and *sodB192*–Hfq–RyhB complexes, respectively. (**B**) Samples containing Hfq alone (lane 1), *sodB192* RNA alone (lane 2) or with RyhB (lane 3) as well as its complexes with Hfq in the absence (lane 4) or presence (lane 5) of RyhB were analysed on a 6% native polyacrylamide gel as described in Materials and Methods (left) followed by western blot analysis using anti-Hfq antibodies (right). Single and double asterisks indicate the *sodB192*–Hfq and *sodB192*–Hfq–RyhB complexes, respectively. (**C**) Radioactively labelled RyhB was incubated alone (lane 1), or with increasing quantities of *sodB192* RNA (1-, 2-, 4- and 8-fold molar excess; lanes 2–5, respectively) or with the equivalent amount of Hfq in the absence (lane 6) or presence (lane 7) of 1-fold molar excess of *sodB192* RNA. Lanes 8–10 correspond to samples containing the pre-formed ternary complex (shown in lane 7), which was further incubated with a 2-, 4- or 8-fold excess of *sodB192* RNA, respectively. The resulting complexes were analysed on a 6% native polyacrylamide gel as described in Materials and Methods. Single and double circles indicate the RyhB–*sodB192* and RyhB–Hfq–*sodB192* complexes, respectively.

of RyhB. We additionally found that the rates of RyhB decay in the wild-type *E.coli* strain and in an *rne*^{ts} mutant are indistinguishable at non-permissive temperature (Figure 6A), suggesting that the above increase in the steady-state level of RyhB (42) does not stem from RyhB stabilization, but instead may be a consequence of transcriptional regulation. For example, the elevated level of RyhB could be, al least in part, brought about by a higher level of Hfq in the *rne*^{ts} mutant (see Figure 6C), which is known to decrease the intracellular concentration of Fur (17), thereby facilitating RyhB transcription.

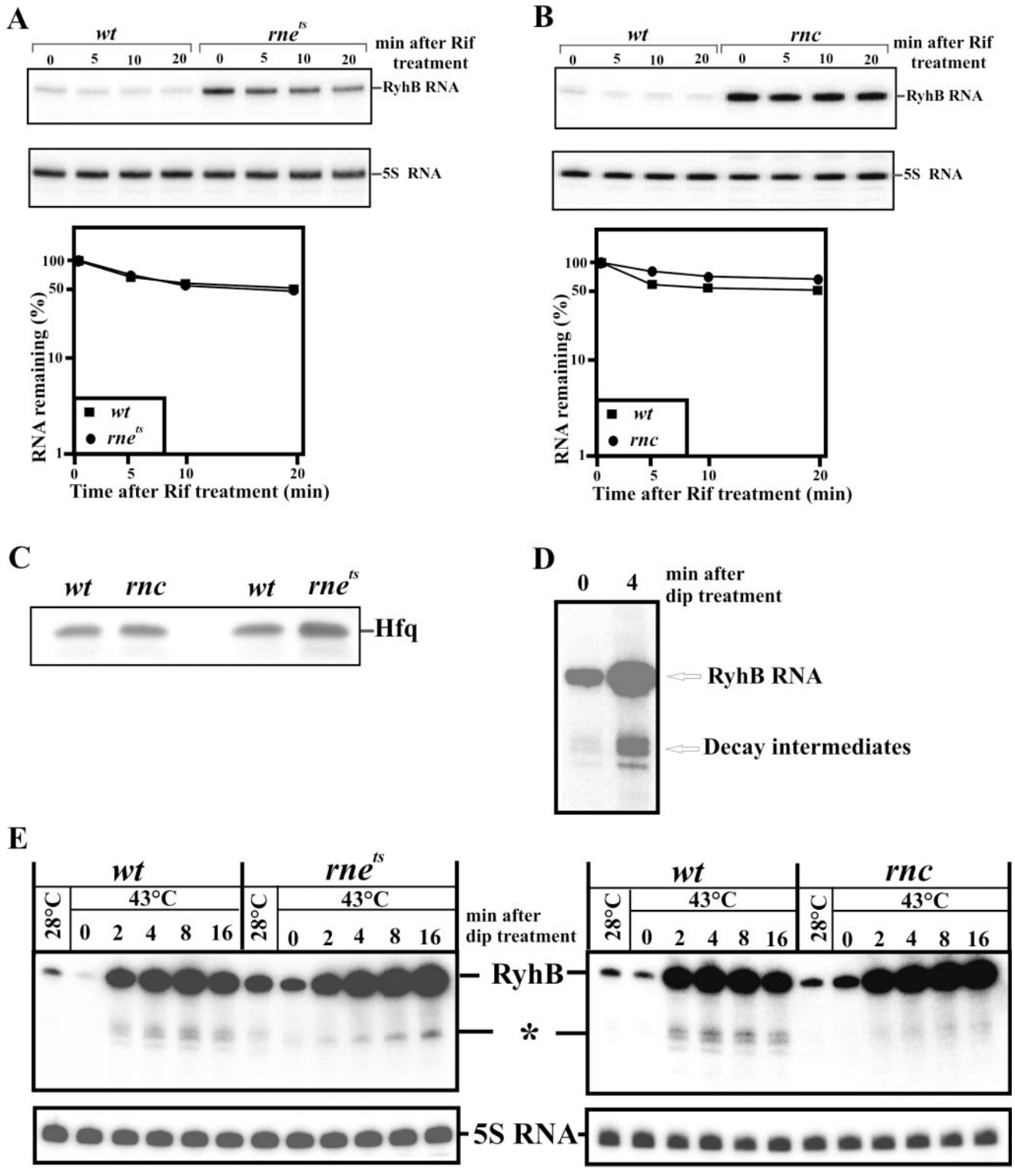

Figure 6. Effects of RNase E and RNase III inactivation on RyhB stability *in vivo*. (**A** and **B**) RNA samples prepared from wild-type *E.coli* cells (*wt*) and their isogenic RNase E (*rne*) and RNase III (*rnc*) mutants at various time points before and after rifampicin treatment were analysed by northern blotting using probes specific for RyhB and 5S rRNA. The latter was employed as an internal standard for normalization of RyhB-specific signals. The graph at the bottom of each panel shows the relative amount of RyhB remaining at each time point as determined by phosphorimaging and plotted as a function of time. (**C**) Equal amounts of total protein cell extracts prepared from wild-type *E.coli* cells (*wt*) and their isogenic RNase E (*rne*) or RNase III (*rnc*) mutants were fractionated on a 15% SDS–polyacrylamide gel followed by western blot analysis using anti-Hfq antibodies. The position of Hfq is indicated. (**D**) RNA samples prepared from wild-type *E.coli* cells before (0) and after (4) 2,2′-dipyridyl treatment (dip) at 28°C were analysed by northern blotting using a probe specific for RyhB. An asterisk indicates the position of RyhB decay intermediates. (**E**) RNA samples prepared from wild-type *E.coli* cells (*wt*) and their isogenic RNase E (*rne*) and RNase III (*rnc*) mutants at various time points before and after 2,2′-dipyridyl treatment (dip) were analysed by northern blotting using probes specific for RyhB and 5S rRNA. The latter was employed as an internal loading control. The molar ratio of Hfq:RyhB was 8:1, respectively. An asterisk indicates the position of RyhB decay intermediates.

Given that RyhB is apparently targeted for degradation via an RNase E-independent pathway, we also investigated whether the absence of functional RNase III, a double-strand specific *E.coli* endoribonuclease [reviewed in (43)], affects the stability of RyhB *in vivo*. Figure 6B shows that the decay rate of RyhB was slightly decreased in an RNase III-deficient strain, indicating that although the main fraction of this transcript still remained unaffected, yet some portion of it seems to be cleaved by this endoribonuclease *in vivo*. While testing this idea further, we found that RyhB degradative intermediates can be easily detected *in vivo* when *E.coli* cell cultures are treated with 2,2′-dipyridyl (Figure 6D). Moreover, their accumulation is not affected by inactivation of RNase E (Figure 6E) but is impaired in an RNase III-deficient strain (Figure 6E). Collectively, these data suggest that RyhB degradation *in vivo* involves its cleavage by RNase III.

RNase III cleavage of RyhB is facilitated by base pairing with its mRNA target

Our *in vivo* data (Figure 6) and the reported interdependence of RyhB and *sodB* mRNA decay (42) suggest that a 9 bp region, which is formed upon RyhB-*sodB* 5′-UTR base pairing (see Figure 7B) (28), together with other double-stranded RNA structures of RyhB can be potentially used by RNase III to bind to the RyhB–*sodB* 5′-UTR complex and to cleave RyhB, thereby targeting it for degradation. To test whether RNase III cleavage of RyhB can be detected *in vitro*, we incubated 5′ end-labelled RyhB with RNase III in the presence of Hfq and increasing quantities of *sodB192* RNA. As shown in Figure 7A, RyhB alone is relatively resistant to RNase III cleavage (lanes 3–5). In contrast, an increase in the concentration of *sodB192* facilitates RNase III cleavage of RyhB at U_{46} and at some minor sites (Figure 7A). Taken together, our *in vivo* and *in vitro* data (Figures 6 and 7, respectively) strongly suggest that the second major *E.coli* endoribonuclease RNase III is involved in RyhB turnover and, therefore, plays an indirect role in RyhB-mediated decay of the *sodB* transcript.

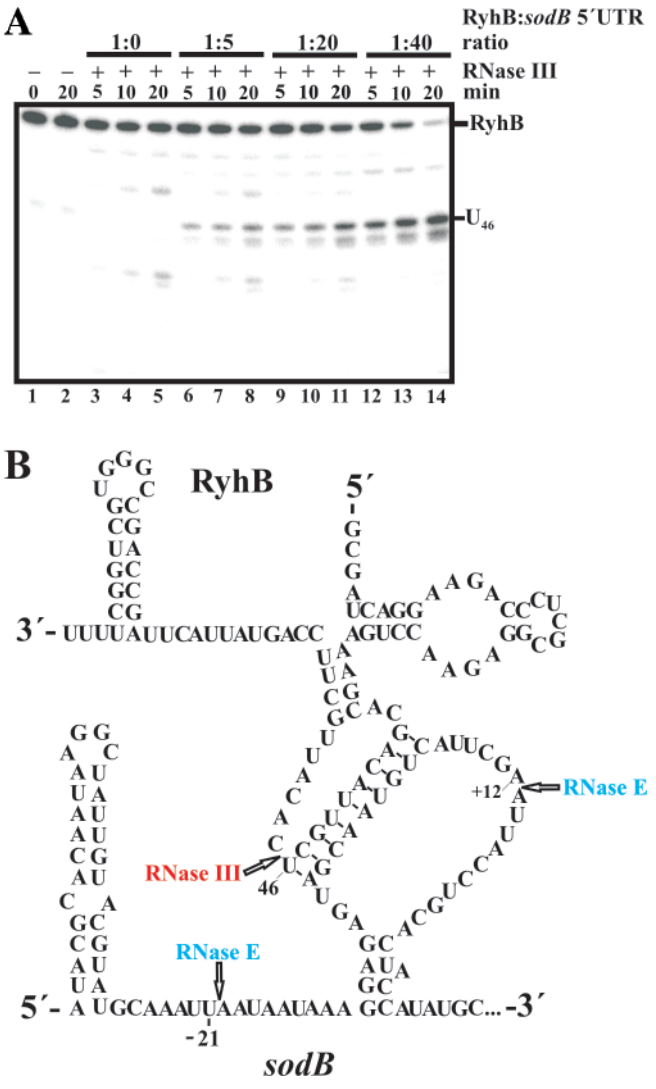

Figure 7. RNase III cleavage of RyhB is stimulated by base pairing with its mRNA target. (**A**) Radioactively labelled RyhB pre-incubated with a 6-fold molar excess of Hfq was further incubated with RNase III in the absence (lanes 1–5) or presence of increasing quantities of *sodB192* RNA (5-, 20- and 40-fold molar excess; lanes 6–14, respectively), and aliquots withdrawn at times indicated above each lane were analysed on a 6% (w/v) polyacrylamide sequencing-type gel. The major nucleotide (U_{46}) at which RNase III cleaves RyhB RNA was determined from concomitantly run S1 and T1 digests of the same RNA (data not shown). (**B**) Model for *sodB* mRNA–RyhB interaction adopted from Geissmann and Touati (28). The major RNase III site of RyhB [see (A)] and RNase E cleavage sites within the 5′-leader of the *sodB* transcript (this study) are shown.

CONCLUSIONS

It is generally believed that the majority of *E.coli* mRNAs are targeted for degradation following initial endonucleolytic cleavages, which often occur within their 5′-UTR (4). In agreement with this model, we demonstrated that decay of *sodB* mRNA is retarded upon inactivation of RNase E *in vivo* (Figure 2) and RNase E cleaves within the 5′-UTR of this transcript *in vitro* (Figure 3). As depicted in Figure 8 (left panel), by eliminating the 5′-end stem–loop structure of the transcript containing the 5′-triphosphate group of the *sodB* transcript, the initial cleavage(s) should render 5′-monophosphorylated intermediate products. As RNA substrates bearing 5′-monophosphate groups are known to be better substrate than triphosphorylated ones for *E.coli* RNase E (44,45) and poly(A) polymerase I (46), the initial cleavage can apparently facilitate the action of these enzymes at subsequent steps of mRNA turnover. In addition to the above role, RNase E cleavage at position U_{-21} reduces the affinity of the *sodB* translation initiation region for ribosomes. Given that a decrease of ribosome loading onto a transcript is known to destabilize the entire mRNA (18,47–49) resulting in its complete decay, our data suggest that functional and chemical inactivation of the *sodB* mRNA are interdependent and are both initiated by RNase E cleavage.

Besides general mechanisms controlling mRNA decay in bacteria, the stability of many transcripts is regulated by environmental factors, such as temperature (50–52), pH (53) and the availability of various chemicals important for bacterial growth and survival (54). Previous work has shown that, during adjustments of *E.coli* to decreasing concentrations of iron, the level of *sodB* mRNA is decreased (55). This regulation involves translational inhibition of *sodB* mRNA by RyhB (17,23,42). We observed that *sodB*/RyhB base pairing

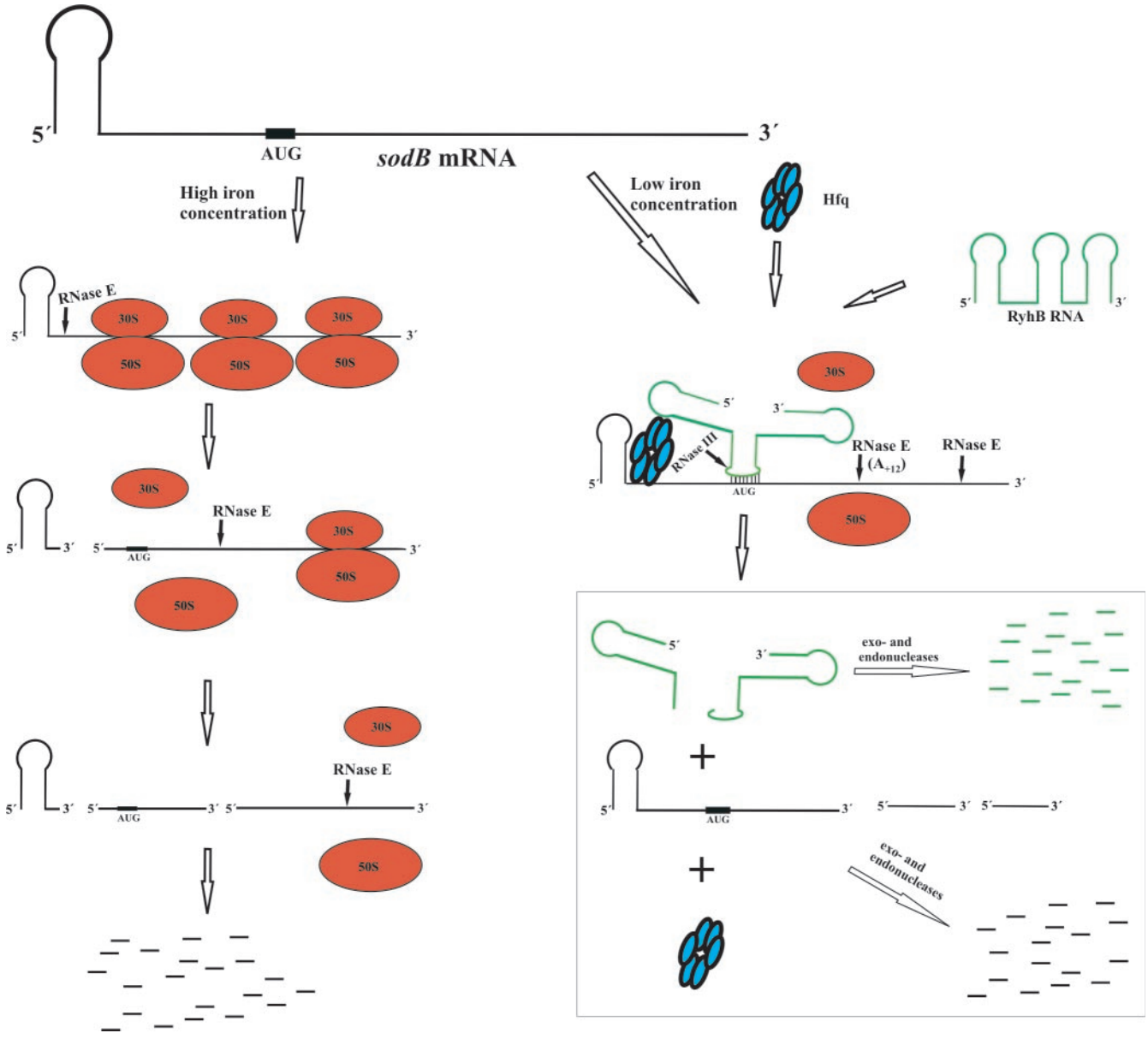

Figure 8. Model for *sodB* mRNA decay at high and low iron concentrations. The pathway for *sodB* mRNA decay in the presence of steady-state levels of iron is shown on the left. The RNase E cleavage eliminates the 5′ terminal stem–loop structure and triggers both chemical and functional inactivation of the transcript. Owing to lower affinity for 30S ribosomal subunits, translation of the truncated *sodB* mRNA is less efficient, thereby allowing RNase E cleavage at downstream site(s). The latter results in the subsequent loss of ribosomal subunits and degradation of the intermediate ribosome-free RNA fragments by endo- and exonucleases. The iron-dependent inactivation of the *sodB* transcript, which is initiated by the small regulatory RNA RyhB and Hfq, is shown on the right. The base pairing with RyhB, which is known to cause structural rearrangements within the *sodB* 5′-UTR (28), inhibits translation and induces RNase E cleavage at the downstream site A_{+12}, whereas the coordinated decay of RyhB is initiated by RNase III cleavage at U_{46} (for details, see Figure 7). Similar to the general pathway, the degradation of the intermediate products is accomplished by exo- and endoribonucleases.

promotes RNase E cleavage at position A_{+12}, i.e. in the immediate coding region of the *sodB* transcript (Figure 8, right panel). This cleavage most likely results from structural rearrangements in the 5′-UTR of *sodB* mRNA upon interaction with Hfq and RyhB. Moreover, although after base pairing of these RNAs Hfq remained associated with the RyhB–*sodB* mRNA complex, it could be released from it through interaction with other ligands. Thus, titration of Hfq by other ligands could free the RNA chaperone from 'death end' complexes.

Finally, although *E.coli* RNase E is often considered as the major enzyme controlling the metabolic stability of mRNA and regulatory RNAs [i.e. RNAI (8)], we showed here that the degradation of RyhB and perhaps that of other sRNAs is not always affected by this enzyme *in vivo* but is dependent on RNase III (Figure 6) known to be involved in rRNA processing and stability control of certain mRNAs (56). Moreover, RNase III cleavage of RyhB was also observed *in vitro* under conditions facilitating RyhB–*sodB* 5′-UTR base pairing, thus suggesting a role for RNase III in the coupled degradation of these transcripts *in vivo*. These data together with another example of post-transcriptional control mediated by the small regulatory RNA IstR (57), which is cleaved by RNase III upon

its base pairing with mRNA, suggest that *E.coli* RNase III may play a much more significant role in bacterial gene regulation.

ACKNOWLEDGEMENTS

The authors are grateful to Donald Court (National Cancer Institute, USA) for providing strains SDF204 and SDF205. This work was supported by grants F1701 and F1707 from the Austrian Science Foundation to U.B. and V.R.K., respectively. Funding to pay the Open Access publication charges for this article was provided by the Austrian Science Foundation.

Conflict of interest statement. None declared.

REFERENCES

1. Le Derout,J., Regnier,P. and Hajnsdorf,E. (2002) Both temperature and medium composition regulate RNase E processing efficiency of the *rpsO* mRNA coding for ribosomal protein S15 of *Escherichia coli*. *J. Mol. Biol*., **319**, 341–349.
2. Nilsson,G., Belasco,J.G., Cohen,S.N. and von Gabain,A. (1984) Growth-rate dependent regulation of mRNA stability in *Escherichia coli*. *Nature*, **312**, 75–77.
3. Vytvytska,O., Jakobsen,J.S., Balcunaite,G., Andersen,J.S., Baccarini,M. and von Gabain,A. (1998) Host factor I, Hfq, binds to *Escherichia coli ompA* mRNA in a growth rate dependent fashion and regulates its stability. *Proc. Natl Acad. Sci. USA*, **95**, 14118–14123.
4. Coburn,G.A. and Mackie,G.A. (1999) Degradation of mRNA in *Escherichia coli*: an old problem with some new twists. *Prog. Nucleic Acid Res. Mol. Biol*., **62**, 55–108.
5. Lundberg,U., Kaberdin,V. and von Gabain,A. (1999) The mechanisms of mRNA degradation in bacteria and their implication for stabilization of heterologous transcripts. In Demain,A.L., Davies,R.M., Cohen,G., Hershberg,C.L., Sherman,D.H., Willson,R.C. and Wu,J.-H.D. (eds), *Manual of Industrial Microbiology and Biotechnology, 2nd edn*. ASM Press, Washington, DC, pp. 585–596.
6. Regnier,P. and Grunberg-Manago,M. (1989) Cleavage by RNase III in the transcripts of the *metY-nusA-intB* operon of *E.coli* releases the tRNA and initiates the decay of the downstream mRNA. *J. Mol. Biol*., **210**, 293–302.
7. Melefors,O. and von Gabain,A. (1988) Site-specific endonucleolytic cleavages and the regulation of stability of *E.coli ompA* mRNA. *Cell*, **52**, 893–901.
8. Lin-Chao,S. and Cohen,S.N. (1991) The rate of processing and degradation of antisense RNAI regulates the replication of ColE1-type plasmids *in vivo*. *Cell*, **65**, 1233–1242.
9. Ehretsmann,C.P., Carpousis,A.J. and Krisch,H.M. (1992) Specificity of *Escherichia coli* endoribonuclease RNase E: *in vivo* and *in vitro* analysis of mutants in a bacteriophage T4 mRNA processing site. *Genes Dev*., **6**, 149–159.
10. Jain,C. and Belasco,J.G. (1995) RNase E autoregulates its synthesis by controlling the degradation rate of its own messenger RNA in *Escherichia coli*: unusual sensitivity of the *rne* transcript to RNase E activity. *Genes Dev*., **9**, 84–96.
11. Portier,C., Dondon,L., Grunberg-Manago,M. and Regnier,P. (1987) The first step in the functional inactivation of the *Escherichia coli* polynucleotide phosphorylase messenger is a ribonuclease III processing at the 5′ end. *EMBO J*., **6**, 2165–2170.
12. Alifano,P., Rivellini,F., Piscitelli,C., Arraiano,C.M., Bruni,C.B. and Carlomagno,M.S. (1994) Ribonuclease E provides substrates for ribonuclease P-dependent processing of a polycistronic messenger RNA. *Genes Dev*., **8**, 3021–3031.
13. Ghosh,S. and Deutscher,M.P. (1999) Oligoribonuclease is an essential component of the mRNA decay pathway. *Proc. Natl Acad. Sci. USA*, **96**, 4372–4377.
14. Iost,I. and Dreyfus,M. (1994) mRNAs can be stabilized by DEAD-box proteins. *Nature*, **372**, 193–196.
15. Moll,I., Afonyushkin,T., Vytvytska,O., Kaberdin,V.R. and Blasi,U. (2003) Coincident Hfq binding and RNase E cleavage sites on mRNA and small regulatory RNAs. *RNA*, **9**, 1308–1314.
16. Py,B., Higgins,C.F., Krisch,H.M. and Carpousis,A.J. (1996) A DEAD-box RNA helicase in the *Escherichia coli* RNA degradosome. *Nature*, **381**, 169–172.
17. Vecerek,B., Moll,I., Afonyushkin,T., Kaberdin,V.R. and Bläsi,U. (2003) Interaction of the RNA chaperone Hfq with mRNAs: direct and indirect roles of Hfq in iron metabolism of *Escherichia coli*. *Mol. Microbiol*., **50**, 897–909.
18. Vytvytska,O., Moll,I., Kaberdin,V.R., von Gabain,A. and Blasi,U. (2000) Hfq (HF1) stimulates ompA mRNA decay by interfering with ribosome binding. *Genes Dev*., **14**, 1109–1118.
19. Masse,E., Majdalani,N. and Gottesman,S. (2003) Regulatory roles for small RNAs in bacteria. *Curr. Opin. Microbiol*., **6**, 324.
20. Masse,E., Escorcia,F.E. and Gottesman,S. (2003) Coupled degradation of a small regulatory RNA and its mRNA targets in *Escherichia coli*. *Genes Dev*., **17**, 2374–2383.
21. Simons,R.W. and Kleckner,N. (1988) Biological regulation by antisense RNA in prokaryotes. *Annu. Rev. Genet*., **22**, 567–600.
22. Sakamoto,H. and Touati,D. (1984) Cloning of the iron superoxide dismutase gene (*sodB*) in *Escherichia coli* K-12. *J. Bacteriol*., **159**, 418–420.
23. Masse,E. and Gottesman,S. (2002) A small RNA regulates the expression of genes involved in iron metabolism in *Escherichia coli*. *Proc. Natl Acad. Sci. USA*, **99**, 4620–4625.
24. Hantke,K. (2001) Iron and metal regulation in bacteria. *Curr. Opin. Microbiol*., **4**, 172–177.
25. Zhang,A., Wassarman,K.M., Ortega,J., Steven,A.C. and Storz,G. (2002) The Sm-like Hfq protein increases OxyS RNA interaction with target mRNAs. *Mol. Cell*, **9**, 11–22.
26. Sledjeski,D.D., Whitman,C. and Zhang,A. (2001) Hfq is necessary for regulation by the untranslated RNA DsrA. *J. Bacteriol*., **183**, 1997–2005.
27. Majdalani,N., Chen,S., Murrow,J., St John,K. and Gottesman,S. (2001) Regulation of RpoS by a novel small RNA: the characterization of RprA. *Mol. Microbiol*., **39**, 1382–1394.
28. Geissmann,T.A. and Touati,D. (2004) Hfq, a new chaperoning role: binding to messenger RNA determines access for small RNA regulator. *EMBO J*., **23**, 396–405.
29. Carpousis,A.J. (2003) Degradation of targeted mRNAs in *Escherichia coli*: regulation by a small antisense RNA. *Genes Dev*., **17**, 2351–2355.
30. Goldblum,K. and Apirion,D. (1981) Inactivation of the ribonucleic acid-processing enzyme ribonuclease E blocks cell division. *Cell*, **15**, 1055–1066.
31. Miczak,A. and Apirion,D. (1993) The *rne* gene and ribonuclease E. *Biochimie*, **75**, 473–479.
32. Dasgupta,S., Fernandez,L., Kameyama,L., Inada,T., Nakamura,Y., Pappas,A. and Court,D.L. (1998) Genetic uncoupling of the dsRNA-binding and RNA cleavage activities of the *Escherichia coli* endoribonuclease RNase III—the effect of dsRNA binding on gene expression. *Mol. Microbiol*., **28**, 629–640.
33. Sonnleitner,E., Moll,I. and Blasi,U. (2002) Functional replacement of the *Escherichia coli hfq* gene by the homologue of *Pseudomonas aeruginosa*. *Microbiology*, **148**, 883–891.
34. Dunn,J.J. and Studier,F.W. (1983) Complete nucleotide sequence of bacteriophage T7 DNA and the locations of T7 genetic elements. *J. Mol. Biol*., **166**, 477–535.
35. Yanisch-Perron,C., Vieira,J. and Messing,J. (1985) Improved M13 phage cloning vectors and host strains: nucleotide sequences of the M13mp18 and pUC19 vectors. *Gene*, **33**, 103–119.
36. Kaberdin,V.R., Chao,Y.H. and Lin-Chao,S. (1996) RNase E cleaves at multiple sites in bubble regions of RNA I stem loops yielding products that dissociate differentially from the enzyme. *J. Biol. Chem*., **271**, 13103–13109.
37. Lin-Chao,S. and Bremer,H. (1986) Effect of the bacterial growth rate on replication control of plasmid pBR322 in *Escherichia coli*. *Mol. Gen. Genet*., **203**, 143–149.
38. Vassilieva,I.M., Rouzanov,M.V., Zelinskaya,N.V., Moll,I., Blasi,U. and Garber,M.B. (2002) Cloning, purification, and crystallization of a bacterial gene expression regulator—Hfq protein from *Escherichia coli*. *Biochemistry*, **67**, 1293–1297.
39. Kaberdin,V.R., Walsh,A.P., Jakobsen,T., McDowall,K.J. and von Gabain,A. (2000) Enhanced cleavage of RNA mediated by an interaction between substrates and the arginine-rich domain of *E.coli* ribonuclease E. *J. Mol. Biol*., **301**, 257–264.

40. Miczak,A., Kaberdin,V.R., Wei,C.L. and Lin-Chao,S. (1996) Proteins associated with RNase E in a multicomponent ribonucleolytic complex. *Proc. Natl Acad. Sci. USA*, **93**, 3865–3869.
41. Hartz,D., McPheeters,D.S. and Gold,L. (1989) Selection of the initiator tRNA by *Escherichia coli* initiation factors. *Genes Dev.*, **3**, 1899–1912.
42. Masse,E., Escorcia,F.E. and Gottesman,S. (2003) Coupled degradation of a small regulatory RNA and its mRNA targets in *Escherichia coli*. *Genes Dev.*, **17**, 2374–2383.
43. Court,D.L. (1993) RNA processing and degradation by RNase III. In Belasco,J.G. and Brawerman,G. (eds), *Control of Messenger RNA Stability*. Academic Press, NY, pp. 71–116.
44. Mackie,G.A., Genereaux,J.L. and Masterman,S.K. (1997) Modulation of the activity of RNase E *in vitro* by RNA sequences and secondary structures 5′ to cleavage sites. *J. Biol. Chem.*, **272**, 609–616.
45. Mackie,G.A. (1998) Ribonuclease E is a 5′-end-dependent endonuclease. *Nature*, **395**, 720–723.
46. Feng,Y. and Cohen,S.N. (2000) Unpaired terminal nucleotides and 5′ monophosphorylation govern 3′ polyadenylation by *Escherichia coli* poly(A) polymerase I. *Proc. Natl Acad. Sci. USA*, **97**, 6415–6420.
47. Iost,I. and Dreyfus,M. (1995) The stability of *Escherichia coli lacZ* mRNA depends upon the simultaneity of its synthesis and translation. *EMBO J.*, **14**, 3252–3261.
48. Joyce,S.A. and Dreyfus,M. (1998) In the absence of translation, RNase E can bypass 5′ mRNA stabilizers in *Escherichia coli*. *J. Mol. Biol.*, **282**, 241–254.
49. Yarchuk,O., Iost,I. and Dreyfus,M. (1991) The relation between translation and mRNA degradation in the *lacZ* gene. *Biochimie*, **73**, 1533–1541.
50. Afonyushkin,T., Moll,I., Bläsi,U. and Kaberdin,V.R. (2003) Temperature-dependent stability and translation of *Escherichia coli ompA* mRNA. *Biochem. Biophys. Res. Commun.*, **311**, 604–609.
51. Johansson,J., Mandin,P., Renzoni,A., Chiaruttini,C., Springer,M. and Cossart,P. (2002) An RNA thermosensor controls expression of virulence genes in *Listeria monocytogenes*. *Cell*, **110**, 551–561.
52. Morita,M.T., Tanaka,Y., Kodama,T.S., Kyogoku,Y., Yanagi,H. and Yura,T. (1999) Translational induction of heat shock transcription factor sigma32: evidence for a built-in RNA thermosensor. *Genes Dev.*, **13**, 655–665.
53. Ang,S., Lee,C.Z., Peck,K., Sindici,M., Matrubutham,U., Gleeson,M.A. and Wang,J.T. (2001) Acid-induced gene expression in *Helicobacter pylori*: study in genomic scale by microarray. *Infect. Immun.*, **69**, 1679–1686.
54. Bernstein,J.A., Khodursky,A.B., Lin,P.H., Lin-Chao,S. and Cohen,S.N. (2002) Global analysis of mRNA decay and abundance in *Escherichia coli* at single-gene resolution using two-color fluorescent DNA microarrays. *Proc. Natl Acad. Sci. USA*, **99**, 9697–9702.
55. Simons,R.S., Jackett,P.S., Carroll,M.E. and Lowrie,D.B. (1976) Superoxide independence of paraquat toxicity in *Escherichia coli*. *Toxicol. Appl. Pharmacol.*, **37**, 271–280.
56. Nicholson,A. (1997) *Escherichia coli* ribonucleases: paradigms for understanding cellular RNA metabolism and regulation. In D'Alessio,G. and Riordan,J.F. (eds), *Ribonucleases: Structures and Functions.* Academic Press, Inc., NY, pp. 38–49.
57. Vogel,J., Argaman,L., Wagner,E.G. and Altuvia,S. (2004) The small RNA IstR inhibits synthesis of an SOS-induced toxic peptide. *Curr. Biol.*, **14**, 2271–2276.
58. Hartz,D., McPheeters,D.S., Green,L. and Gold,L. (1991) Detection of *Escherichia coli* ribosome binding at translation initiation sites in the absence of tRNA. *J. Mol. Biol.*, **218**, 99–105.